Dynamic updating of spatial working memory across eye movements: a computational investigation of transsaccadic integration

Sijia Zhao[1,‡,*], Thomas Parr[2,‡], Rob Udale[1], Verena Klar[1], Gabriel David Jones[2,3], Anna Scholcz[1,2], Sofia Toniolo[2,4], Sanjay G. Manohar[1,2,4], Masud Husain[1,2,4]

1 Department of Experimental Psychology, University of Oxford, Oxford OX2 6GG, UK
2 Nuffield Department of Clinical Neurosciences, University of Oxford, Oxford OX3 9DU, UK
3 Nuffield Department of Women's and Reproductive Health, University of Oxford, Oxford OX3 9DU, UK
4 Cognitive Disorders Clinic, John Radcliffe hospital, University of Oxford, Oxford OX3 9DU, UK

‡ SZ and TP had equal contribution to this paper.

*** Corresponding author:** Sijia Zhao, sijia.zhao@psy.ox.ac.uk, Department of Experimental Psychology, University of Oxford, New Radcliffe House, Radcliffe Observatory Quarter, Oxford OX2 6GG

Author Contributions: S.Z.: Conceptualization, Methodology, Formal analysis, Data Curation, Writing - Original Draft, Writing – Review & Editing, Visualization, Project administration. **T.P.**: Methodology, Formal analysis, Writing - Original Draft, Writing – Review & Editing, Visualization. **R.U.**: Conceptualization, Methodology, Software, Validation, Formal analysis, Investigation, Resources, Data Curation, Project administration. **V.K.:** Methodology, Resources, Investigation, Data Curation, Writing - Review & Editing, Project administration. **G.D.J.**: Resources, Data Curation. **A.S.**: Data Curation. **S.T.**: Conceptualization, Resources, Data Curation, Writing - Review & Editing. **S.M.**: Conceptualization, Methodology, Writing – Review & Editing, Supervision. **M.H.**: Conceptualization, Methodology, Resources, Writing – Review & Editing, Project administration, Supervision, Funding acquisition.

Competing Interest Statement: All authors declare no financial or non-financial competing interests.

Classification: Biological Sciences/Psychological and Cognitive Sciences.

Keywords: remapping, spatiotopic memory, retinotopic memory, drawing, eye movements

Acknowledgement

This research was supported by funding from the Wellcome Trust and National Institute of Health and Care Research (NIHR) Oxford Health Biomedical Research Centre (BRC). S.Z., R.U., V.K., G.D.J., A.S., S.T. and M.H. were funded by the Wellcome Trust (206330/Z/17/Z and 226645/Z/22/Z). S.G.M. was funded by a Medical Research Council (MRC) Clinician Scientist Fellowship (MR/P00878/X), NIHR BRC and NIHR Oxford Health BRC. T.P. is supported by an NIHR Academic Clinical Fellowship (ref: ACF-2023-13-013).

Abstract

The brain continuously integrates rapidly changing visual input across eye movements to maintain stable perception, yet the precise mechanisms underpinning dynamic working memory and how these break down in brain diseases remain unclear. We developed a novel eye-tracking paradigm and computational models to investigate how spatial and colour information are updated across saccades. Our findings reveal that saccades selectively impair spatial but not colour memory. Computational modelling identified that spatial representations are maintained in a dual eye-centred frame of reference which is actively updated by a noisy memory of saccades but is vulnerable to interference. Using this model, we found that specific mechanistic failures in initial encoding and memory decay, rather than the saccadic updating process itself, account for spatial working memory deficits in Alzheimer's and Parkinson's disease. These results provide a mechanistic understanding of how dynamic spatial memory operates in health and its disruption in neurodegenerative disorders.

Introduction

Natural vision is profoundly dynamic, relying upon sequences of saccades. Everyday tasks, such as making a cup of tea [1,2], arranging the layout of objects [3,4], or copying a simple line drawing [5–7], require us to precisely track spatial locations—which appear at different retinotopic locations with each fixation—across saccades [8]. This requires a dynamic updating process, termed "remapping", that involves updating our internal representation of object locations to maintain a stable world-centred frame of reference [9–12]. One key hypothesis is that we use working memory across visual fixations to update perception dynamically [13,14]. However, despite the apparent stability of our visual world, it has proven difficult to separate the distinct contributions of retinal memory from transsaccadic memory. To precisely characterise the interplay of factors contributing to dynamic spatial working memory—particularly amidst the complexities of multiple fixations as well as the potential for memory decay and interference—and to move beyond purely descriptive observations, fundamental questions regarding the underlying mechanisms and sources of potential errors need to be addressed.

Central to such an endeavour is understanding the nature of the brain's internal spatial representation: Is it a single, world-centred (allocentric) map, or does it rely on a fixation-centred (retinotopic) representation that must be actively updated after each saccade [11,13,15,16]? If the latter, how do we keep track of the fixation locations from which the allocentric spatial location can be reconstructed? Do our brains retain memories for recent fixation locations, or do we reconstruct these from memories of recent saccades? One way of addressing these questions is to examine the spatiotemporal patterns of errors made during working memory tasks. Under the assumption that imperfect memory traces are subject to time-dependent decay [17], the patterns of errors made should differ depending upon the spatial variables represented.

In addition to these unresolved questions in healthy people, it has become apparent that neurodegenerative conditions such as Alzheimer's disease (AD) and Parkinson's disease (PD) can be associated with significant disruptions to visuospatial processing and constructional apraxia (a disorder characterised by impaired drawing and copying abilities)[18,19].This raises a crucial question: Could specific deficits in transsaccadic remapping mechanisms explain the impairments in complex visuospatial tasks, such as copying drawings?

To address these questions and move beyond purely descriptive observations towards mechanistic models, we developed a novel eye-tracking paradigm — the LOcation and Colour Updating across Saccades (LOCUS) paradigm (**Figure 1**)—to directly compare

retinotopic and transsaccadic working memory for both spatial location and colour. Combined with computational modelling, our approach allowed us to precisely characterize the interplay of factors contributing to dynamic spatial working memory, isolate the impact of saccades, and test specific, competing hypotheses regarding transsaccadic memory. Including young and older healthy adults as well as patients with Parkinson's and Alzheimer's disease, our findings reveal that saccades selectively disrupt spatial but not colour memory. Across all healthy and patient groups, the winning computational model indicated that spatial representations are maintained in a dual (retinotopic) reference frame, updated based on a noisy memory of the saccade vector, and susceptible to interference from other items in memory. Importantly, we identified specific model parameters—related to angular encoding, memory decay, and interference—that differentiated the patient groups from healthy controls, providing a mechanistic account of their visuospatial deficits.

Results

Saccades disrupt spatial memory but spare colour

In the LOCUS (Location and Colour Updating across Saccades) paradigm (***Figure 1***), participants memorised the colour and location of two sequentially presented squares. Subsequently, they were cued to recall the colour and location of one of these squares, i.e. either the first or the second. Colour recall involved clicking on a colour wheel to indicate the remembered colour using the mouse. Location recall required dragging a colour-matched square to the remembered position on the screen.

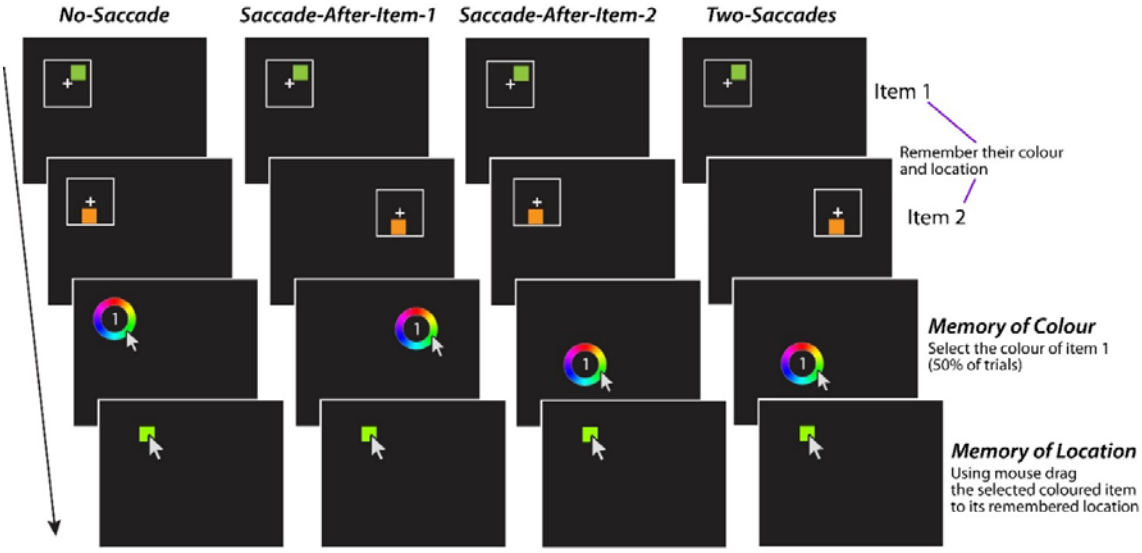

Figure 1: Location and Colour Updating across Saccades (LOCUS) Task.

*Participants were asked to fixate a white cross, wherever it appeared. They had to remember the colour and location of a sequence of two briefly presented coloured squares (Item 1 and 2), each appearing within a white square frame. They then fixated a colour wheel wherever it appeared on the screen. This cued recall of a specific square (Item 1 or Item 2 labelled within the colour wheel). Participants selected the remembered colour on the colour wheel which led to a square of that colour appearing on the screen. They then dragged this square to its remembered location on the screen. There were four conditions: **1**) No-Saccade condition providing a measure of retinotopic memory; **2**) Saccade After Item 1; **3**) Saccade After Item 2; **4**) Saccades after both items (Two Saccades condition). Conditions 2)-4) provide a measure of the impact of 1 or 2 saccades on recall, in addition to any retinotopic contribution.*

By manipulating the spatial location of the squares and also that of the colour wheel, we controlled saccadic demands on every trial, creating four conditions with equal probability: no-saccade, saccade after Item 1, saccade after Item 2 (to the colour wheel), or a saccade after both items. The no-saccade trials provided a measure of retinotopic working memory, while the two-saccade trials assessed transsaccadic working memory. To mitigate potential confounds, we monitored eye position throughout the experiment. Eye-tracking analysis confirmed high compliance: participants correctly maintained fixation or executed saccades as instructed on the vast majority of trials (83% ± 14%). Non-compliant trials were excluded from further analysis.

This design allowed us to isolate and quantify the unique impact of saccades on spatial memory, enabling us to test competing hypotheses regarding spatial representation. If an allocentric mechanism solely underpinned spatial memory, we would anticipate no difference in memory precision across saccade conditions, as the spatial representation would be world-centred and unaffected by eye movements. Thus, performance in the no-saccade condition should be comparable to the two-saccade condition.

Conversely, if spatial memory relies on a retinotopic representation that requires active updating with eye movements, a different pattern or error would be predicted. The two-saccade condition was anticipated to be the most challenging due to cumulative decay in the memory traces used for stimulus reconstruction after each saccade [20]. In contrast, the no-saccade condition was expected to yield the most accurate localisation, relying solely on retinotopic information. Additionally, given well-known recency effects in working memory, recall performance for the second item was also expected to be better than for the first stimulus in each condition [21,22]. This is implicit in all of the models we tested because the variance of responses grows with time since the stimulus was observed. Importantly, we also hypothesised that saccades would selectively disrupt location memory while leaving colour memory intact.

These predictions were confirmed in young healthy adults (N = 21, mean age = 24.1 years, ranged between 19 and 34). A repeated measures ANOVA revealed a significant main effect of saccades on location memory ($F(2.2,43.9)=33.2$, $p<0.001$, partial $\eta^2=0.62$), indicating substantial impairment after eye movements (***Figure 2A***). The saccades affected both items similarly (no interaction between saccades and item ($F(2.6,52.7)=0.64$, $p=0.57$, partial $\eta^2=0.03$). However, as expected, spatial memory for Item 1 was significantly less accurate than for Item 2 ($F(1,20) = 12.5$, $p = 0.002$, partial $\eta^2 = 0.38$). Crucially, even a single saccade after Item 2 significantly reduced location memory accuracy compared to the no-saccade condition ($t=-7.64$, $p(bonf)<0.001$).

Saccadic interference with location memory is particularly striking because even eye movements directed towards the colour wheel to report the colour remembered had a detrimental effect on the preservation of precise spatial representations. In contrast, colour memory itself was not affected by saccades (***Figure 2B***; $F(2.2, 44.7) = 0.68$, $p=0.53$, partial $\eta^2 =0.03$), confirming the specificity of saccadic interference on spatial memory. The expected recency effect was also observed in colour report, with better memory for the second item ($F(1,20) = 6.52$, $p = 0.02$, partial $\eta^2 = 0.25$).

Further analysis indicated that larger saccades were associated with increased spatial memory disruption (see Supplementary Materials for "Larger saccades disrupt memory more"). A multiple linear regression predicting location error showed that only the vertical distance between stimulus frames significantly predicted error ($t(41)=5.73, p<0.0001$), with marginal significance for horizontal saccade direction ($t(41)=-1.94, p=0.059$). This suggests that greater displacement, particularly vertical, exacerbates spatial memory impairment, irrespective of saccade direction. However, there was no evidence that crossing saccades (e.g., rightward then leftward) or specific horizontal/vertical saccade directions differentially affected spatial memory precision, as revealed by repeated measures ANOVAs

(F(1.3,49.8)=0.04, p=0.89, partial η2=0.001 for horizontal crossing; F(1.7,62.8)=0.29,p=0.71, partial η2=0.008 for vertical crossing).

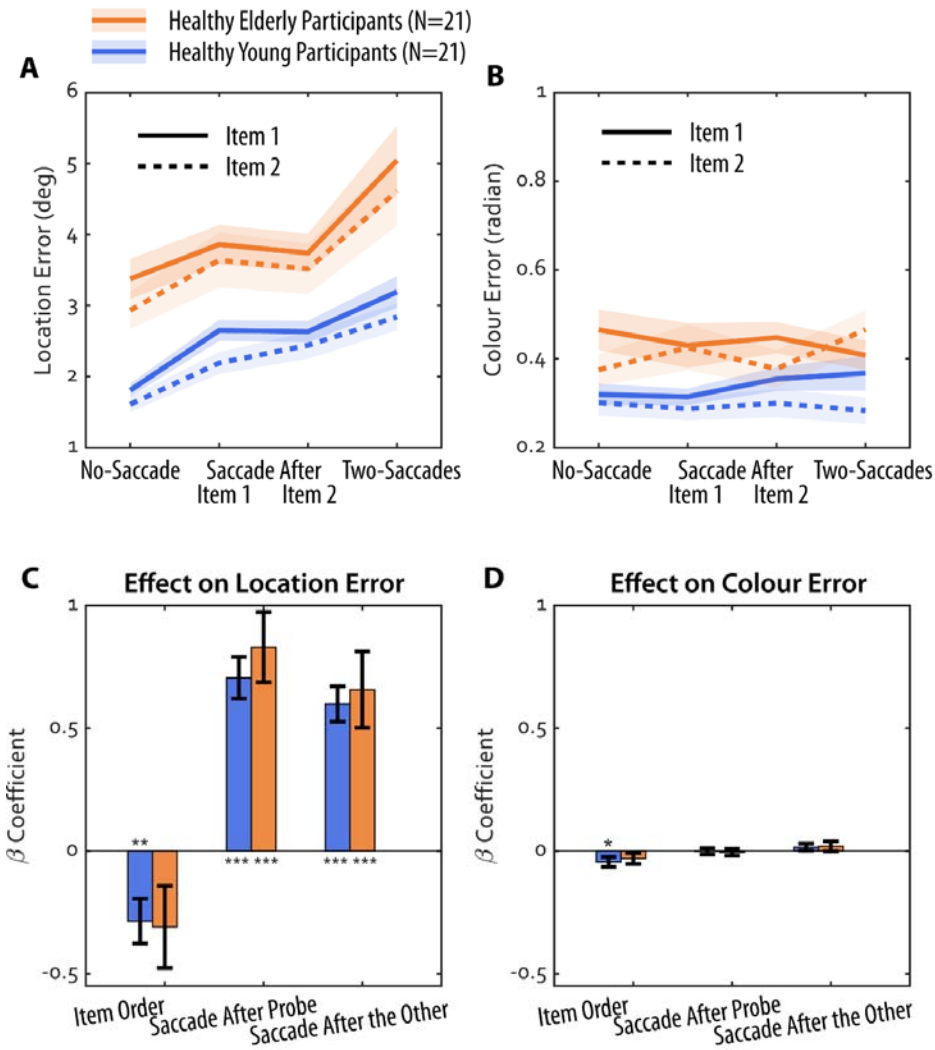

Figure 2: Saccades lead to increased recall error for location but not colour.
(A) *Mean location error for each saccade condition, and for each probed item (Item 1: solid lines; Item 2: dashed lines).* ***(B)*** *Colour error for the same conditions. Shaded error represents ±1 standard error from mean.* ***(C)*** *Beta coefficients from a multiple linear regression model predicting location error, illustrating the effect of item order (1 or 2), saccade after the probed item, and saccade after the other item, for young (blue) and elderly (orange) participants. Error bars represent ± 1 standard errors. (D) The same model applied to colour errors, revealing a recency effect but no impact of saccade demands. ** means significantly different from zero p<0.01, *** means significantly different from zero p<0.001.*

Saccadic interference with spatial memory is age-independent

To investigate the impact of aging, we replicated the experiment in a group of healthy adults above 60 (Elderly Healthy Adults; *N* = 21; mean age = 72.4 years, ranged between 60 and 80). A three-way ANOVA (4 saccade conditions x 2 items x 2 age groups) revealed a main

effect of age, with older participants demonstrating lower overall accuracy compared to their younger counterparts (***Figure 2A***, $F(1,40) = 22.73$, $p < 0.001$, partial $\eta^2 = 0.36$). This age-related decline was evident in both transsaccadic working memory (Two-Saccades Location Error, rho=0.57, $p < 0.001$, Fisher's $z = 0.64$; partial rho=0.55, $p<0.001$, $z=0.62$ after controlling gender and ACE total score) and retinotopic working memory (No-Saccade Location Error, rho=0.70, $p<0.001$, Fisher's $z = 0.86$; partial rho=0.69, $p<0.001$, $z=0.85$).

These findings suggest that while both retinotopic and transsaccadic working memory decline with age, the relative impact of saccades on spatial memory remains stable across age groups. This was also supported by the lack of significant interaction between age group, saccade condition, and item type (all $p > 0.23$), suggesting that the detrimental effect of saccades on spatial memory is constant across both young and older adults. This observation was further supported by post-hoc tests, which confirmed the *same* pattern of location errors across saccade conditions in both groups: the no-saccade condition exhibited the least location error ($p(bonf) < 0.001$, $|t| \geq 5.94$), followed by the one-saccade conditions (no difference between them: $t = 0.02$, $p(bonf) = 1.00$, Cohen's $d = 0.002$), and with the highest error on the two-saccade condition ($|t|\geq3.53$, $p(bonf) \leq 0.006$).

A multiple linear regression model, incorporating data from both age groups further corroborated these findings. Both earlier item presentation and the presence of saccades after either item predicted increased location error (***Figure 2C***) but not colour error (***Figure 2D***). There was no difference in the beta coefficients between two age groups.

In summary, while healthy aging was associated with a general decline in spatial memory accuracy, the specific disruptive effect of saccades on spatial – but not colour – memory remained constant across age groups. Thus, the mechanisms underlying transsaccadic remapping and its impact on spatial working memory are generally preserved in healthy aging, despite an overall reduction in memory performance.

Computational model comparison reveals the mechanisms of transsaccadic memory

To dissect the specific cognitive processes underlying the observed saccade cost on spatial memory, we turned to computational modelling with a suite of seven computational models designed to test specific, competing hypotheses about how the brain represents and updates visual information across saccades (**Table 1**). The models are organised hierarchically, starting from a simple, single-representation model and progressively incorporating more complex mechanisms. This allows us to systematically identify which mechanisms are necessary to account for the observed behaviour. The model, data, and analysis scripts are all available in the open dataset: https://osf.io/95ecp/.

Our modelling framework addresses three core conceptual distinctions:

(1) **Reference frame.** Whether spatial memory is maintained in a single, world-centred (allocentric) map (**Figure 3A**), or relies on a dual, fixation-centred (retinotopic) reference frame (**Figure 3B**).
(2) **Distractor interference.** Whether memory is susceptible to interference from other items held in memory (**Figure 3C**).
(3) **Remapping source.** Within a dual-frame system, whether error arises from a passive decay of the remembered fixation point (**Figure 3D**), or from an active but noisy reconstruction based on the saccade vector itself (**Figure 3E**).

All models assume that memory for location decays over time, formalised as a diffusion (Brownian motion) process, where the precision of the remembered location decreases with increasing retention interval. The key differences between the models lie in what is decaying and when (see Methods for mathematical details and detailed variance functions).

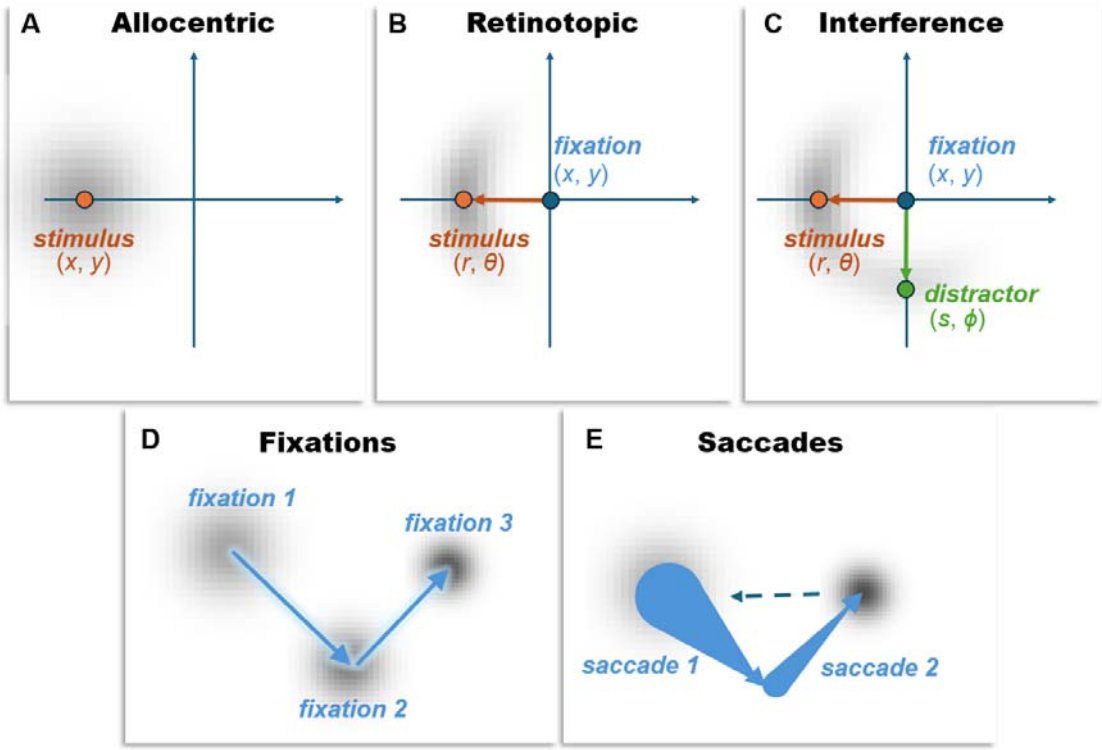

Figure 3: Conceptual illustration of allocentric vs retinotopic spatial representations.
This figure depicts the distinction between various representations of spatial memory. These include allocentric (world-centred) and retinotopic (eye-centred) spatial representation. ***(A)*** *The* ***Allocentric*** *panel illustrates a world-centred reference frame, where a stimulus location (x, y) is represented independently of eye position. The spread of the grey shaded area around the stimulus indicates for this representation the encoding error and subsequent decay since the stimulus was viewed. In this framework, memory error is assumed to increase over time due to a general decay of the stored coordinates, which is treated as a decay in Euclidean space, such that the probability density of a remembered location (coordinates (x,y)) is a normal distribution whose covariance grows with time centred on the stimulus. This model corresponds to Model 1 in Table 1.* ***(B)*** *The* ***Retinotopic*** *panel presents an eye-centred reference frame, where the stimulus location is encoded relative to the current fixation point (x, y) using polar coordinates: radial distance (r) and angular direction (θ). The orange arrow indicates the vector from fixation to the stimulus, representing these encoded retinotopic coordinates. The grey shaded area here again represents the initial encoding error and subsequent decay, which can be decomposed into radial and angular components. This* ***dual model****, incorporating both encoding error and decay in radial and angular components, corresponds to Model 2 in Table 1. It forms the basis for more complex models (Models 3-7 in Table 1) that differentiate between decay of the reference frame itself (e.g., recall of fixation point) and updating based on saccade information.* ***(C)*** *The* ***Interference*** *panel shows the combination of a stimulus and distractor (translated into the same retinotopic coordinates), with some probability associated with a response to the memory of the distractor stimulus. The lower two panels distinguish between whether the origin of the retinotopic plot is recalled based upon a remembered fixation location* ***(D)****, or whether it is based upon a reconstruction after propagating back through remembered saccade vectors* ***(E)*** *— conceptually shown with arrows whose base is large to indicate the (cumulative) uncertainty in the origin points of each vector.*

Index	Model name	Components
1	Allocentric	Allocentric Encoding Error + Allocentric Decay
2	Dual	Radial Encoding Error + Radial Decay + Angular Encoding Error + Angular Decay
3	Dual (Fixation)	Dual + Fixation Decay
4	Dual (Saccade)	Dual + Saccade Encoding Error + Saccade Decay
5	Dual + Interference	Dual + Interference
6	Dual (Fixation) + Interference	Dual + Fixation Decay + Interference
7	Dual (Saccade) + Interference	Dual + Saccade Encoding Error + Saccade Decay + Interference

Table 1: Hypotheses expressed as seven competing models.

These conceptual distinctions give rise to a family of seven specific computational models (**Table 1**):

1. **Allocentric model**: This model assumes the brain stores locations in a single, stable, world-centred (allocentric) reference frame. In this model, memory error arises solely from a time-dependent decay of the stored coordinates, independent of any eye movements.
2. **Dual model**: This foundational model introduces the core hypothesis of a dual-reference frame. It posits that locations are initially encoded in eye-centred (retinotopic) coordinates (**radial** distance and **angular** direction from fixation), which are then subject to both initial encoding errors and time-dependent decay. This forms the basis for more complex models that explicitly distinguish between decay in the reference frame's centre and coordinates within that frame.
3. **Dual (fixation decay) model**: Building on the dual-frame hypothesis, this model proposes that to remap a location after a saccade, the brain uses its memory of the *original fixation point*. This memory trace of the eye's position itself decays over time, introducing a specific source of error into the remapped location. Of note, the time at which the memory of the fixation location starts to decay is the time of the first saccade following the disappearance of the stimulus. This means that, depending upon the experimental condition, the fixation memory starts to decay *after* the retinotopic memories start to decay.
4. **Dual (saccade update) model**: This model offers an alternative updating mechanism. Instead of relying on a memory of the absolute fixation location, it proposes that the brain uses a memory of the *saccade vector* itself (the direction and amplitude of the eye movement). The original location is then reconstructed based on this imperfect, noisy memory of the saccade, providing a different source of remapping error. Here, each saccade between the fixation at which the stimulus was shown and the response time injects an additional encoding error which have cumulative effects, in addition to the cumulative memory decay from decays in each of the saccade vector memories in the time since the saccade.
5. **Dual + interference model**: This model tests the influence of cognitive load by incorporating crosstalk between items in memory. It suggests that the memory for the target location is partially corrupted by the presence of the other, distracting item's location, adding a source of error independent of remapping. In effect, this means the

response distribution is assumed to be a weighted sum between the distributions anticipated if responding to the target or to the distractor.

6. **Dual (fixation decay) + interference model**: This model combines two potential sources of error: the passive decay of the remembered fixation point (Fixation Decay) and corruption from the distractor item (Interference).
7. **Dual (saccade update) + interference model**: This is the most complex model, combining the active, saccade-based updating mechanism with distractor interference. It proposes that memory error arises from both an imperfect remapping process based on a noisy saccade signal and from confusion with the other item held in memory.

By fitting these models to our participants' response data, we inferred which set of mechanisms best explains their performance. We fit all seven models to the trial-by-trial response data from all healthy participants (N=42) (**Figure 4**) and used random-effects Bayesian model selection (BMS) to identify the most plausible generative model, a process that inherently balances model fit with complexity [23–25]. The analysis yielded a strong result: the "**Dual (Saccade) + Interference**" model (**Model 7 in Table 1**) emerged as the winning model, providing substantial evidence against the next best alternative with a Bayes Factor of 6.11. This indicates substantial evidence that saccade-based updating with distractor interference is the most prevalent generative process in the healthy population.

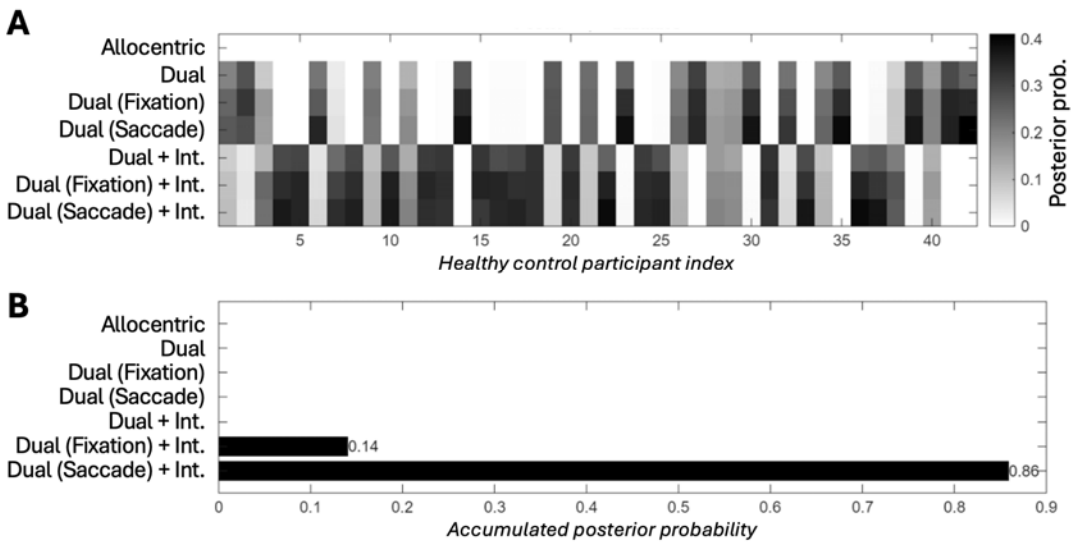

Figure 4: Model comparison results in healthy control (HC) participants (N=42).
(A) *Individual participant posterior probabilities. Heatmap illustrates the posterior probability for each of the seven competing models across individual healthy participants. The red dashed vertical line separates the age groups, with young controls on the left and elderly healthy controls on the right. This panel indicates that the 'Dual (Saccade Update) + Interference' model frequently shows the highest posterior probability for individual participants.* ***(B)*** *Aggregate model posterior probabilities. Bar chart showing the posterior probability for each competing model, aggregated across all healthy participants.*

The superiority of this specific model provides three critical insights. Firstly, the victory of a dual-frame model over the simpler allocentric model strongly supports the hypothesis that spatial memory is fundamentally reliant on eye-centred representations that must be actively updated. Secondly, the model comparison decisively adjudicates the source of remapping error: the clear win for the 'Saccade Update' mechanism suggests that transsaccadic error arises not from a passive forgetting of where the eyes were, but from an active, yet imperfect, process of remapping based on a noisy internal copy of the saccade command—or, perhaps,

from the proprioceptive signal associated with that movement. Finally, the inclusion of the 'Interference' term was essential for the winning model, demonstrating that this remapping process is also susceptible to confusion from other items held in memory. This winning model was therefore used for all subsequent analyses.

Patients with AD and PD show preserved saccadic interference but greater overall error

Having established the mechanisms in healthy individuals, we next investigated how these processes are affected in patients with Alzheimer's disease (AD) and Parkinson's disease (PD), comparing their performance to that of both young (YC) and elderly (EC) controls. As anticipated, there was a significant main effect of group on overall memory performance. A two-way ANOVA revealed that patient groups were less accurate on both location ($F(3, 318) = 59.71$, $p < 0.001$) and colour memory ($F(3, 318) = 47.85$, $p < 0.001$). Post-hoc analyses confirmed that AD patients exhibited significantly greater errors than all other groups across every condition (e.g., on No-Saccade Location Error vs YC, EC, and PD: all $p < 0.001$; see **Figure 5**).

Across all groups, saccades selectively disrupted spatial memory—shown by a significant main effect of condition on location error ($F(3, 318) = 4.64$, $p = 0.003$)—but not on colour error ($F(3, 318) = 0.80$, $p = 0.49$). Most strikingly, the fundamental pattern of saccadic interference seen in healthy controls was fully replicated in the patient cohorts. In other words, the magnitude of this saccadic disruption did not differ between groups. We found no significant interaction between group and condition for either location ($F(9, 318) = 0.46$, $p = 0.90$) or colour memory ($F(9, 318) = 0.26$, $p = 0.98$). This critical null-interaction indicates that while overall spatial precision is lower in patients, the additional computational cost imposed by a saccade is not disproportionately larger.

The pattern of performance decay from the no-saccade to the two-saccade condition was remarkably consistent across all groups (**Figure 5A**), suggesting that the core mechanisms for updating spatial representations across eye movements are surprisingly resilient to the neurodegenerative processes in both PD and AD.

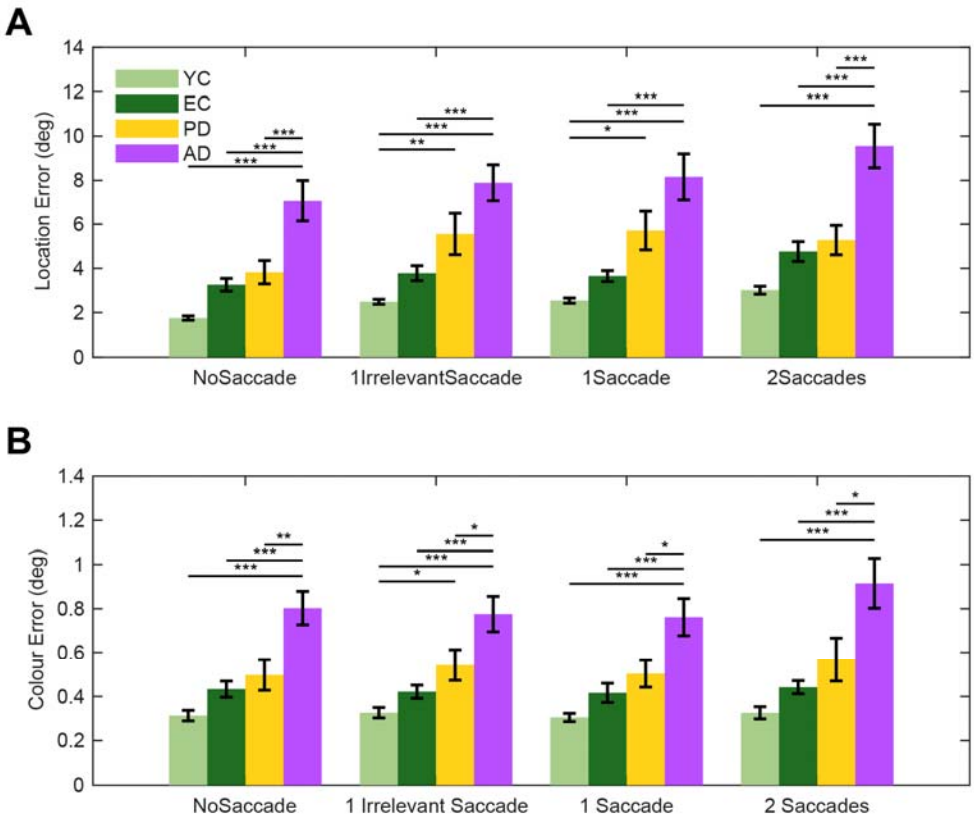

Figure 5: Saccadic interference with spatial memory is preserved across healthy aging and neurodegenerative conditions, despite group differences in recall error.

*Saccades lead to increased recall error for location, but not colour, in healthy young (YC) and elderly (EC) controls, as well as in patients with PD and AD. While patient groups exhibit greater overall memory errors, the fundamental pattern of saccadic disruption remains consistent across all cohorts. (**A**) Location error. Mean location error (in degrees of visual angle) for each saccade condition (No-Saccade, 1 Irrelevant Saccade, 1 Saccade, 2 Saccades) for all participant groups. A two-way ANOVA revealed a significant main effect of Group and Condition, but there was no significant Group × Condition interaction ($F(9, 318) = 0.46$, $p = 0.900$), indicating that the magnitude of saccadic disruption to spatial memory is constant across groups. Post-hoc Tukey-Kramer comparisons within each condition between groups confirmed a graded impairment in overall spatial accuracy: AD patients exhibited significantly greater errors than all other groups (e.g., AD vs. YC, EC, PD: all $p < 0.001$), PD patients performed worse than both YC and EC (all $p < 0.001$), and EC performed worse than YC (all $p < 0.001$). The significant post-hoc between group comparisons are shown above the bar plots, with Bonferroni multiple comparison correction applied. (**B**) Colour error. Mean colour error (in radians) for each saccade condition across participant groups. For colour memory, a two-way ANOVA revealed a significant main effect of* Group *but no significant main effect of Condition or Group × Condition interaction. Post-hoc comparisons for colour error showed a similar pattern of overall group differences as observed for location memory (all group comparisons $p < 0.001$). Error bars represent ±1 standard error of the mean (SEM). Asterisks denote statistical significance from post-hoc comparisons: *: p<0.05, **: p<0.01; ***: p<0.001.*

Modelling reveals the sources of spatial memory deficits in AD and PD

To understand the source of the patients' deficits, we applied the winning 'Dual (Saccade) + Interference' model the data from all participants (YC, EC, AD, and PD). By fitting the model

to the entire dataset, we obtained estimates of the parameters for each individual, which then formed the basis for our group-level analysis. To formally test for group differences, we used Parametric Empirical Bayes (PEB), a hierarchical Bayesian approach that compares parameter estimates across groups while accounting for the uncertainty of each estimate [26]. This allowed us to identify which specific cognitive mechanisms, as formalised by the model parameters, were affected in the patient cohorts.

The analysis revealed a nuanced pattern of deficits, with four parameters differentiating the groups (**Figure 6**). The most prominent deficits were observed in memory decay and interference. The Bayesian inversion used here allows us to quantify the posterior mode and variance for each parameter and the covariance for each parameter. From these, we can compute the probabilities that pairs of parameters differ from one another, which we report as P(A>B)—meaning the posterior probability that the parameter for group A was greater than that for group B.

Radial decay showed a clear, graded impairment: AD patients had a greater decay rate than PD patients (P(AD > PD) = 1.000), who in turn were more impaired than EC (P(PD > EC) = 0.996), and who were more impaired than YC (P(EC > YC) = 0.995). A similar graded pattern was observed for Interference, where AD patients were most susceptible (P(AD > PD) = 0.999), followed by EC (P(EC > YC) = 1.000), while PD and EC groups did not significantly differ (P(PD > EC) = 0.532). Patients with AD also showed a tendency towards greater angular decay than controls (P(AD > YC) = 0.924; P(AD > EC) = 0.772), although this fell below 95% probability. This effect was partly influenced by a surprisingly lower decay rate in the PD group compared to EC (P(PD < EC) = 0.037, indicating P(EC > PD) = 0.963), but not YC (P(PD < YC) = 0.140).

In contrast, group differences in encoding were less pronounced. Only angular encoding error significantly (applying a 95% threshold) differentiated the groups, an effect largely driven by the particularly high precision of the YC group compared to AD (P(YC < AD) = 0.000), PD (P(YC < PD) = 0.019), and EC (P(YC < EC) = 0.002). Among the patient and elderly control groups, AD showed significantly higher angular encoding error than PD (P(AD > PD) = 0.985), but AD and PD did not significantly differ from EC (P(AD > EC) = 0.909; P(PD > EC) = 0.787).

Crucially, and in line with our behavioural findings, parameters related to the saccade itself—saccade encoding and saccade decay—did not differentiate between groups. This modelling result reinforces the conclusion that the core computational process of updating spatial information based on an eye movement is not the primary locus of impairment in PD or AD. Instead, this approach pinpoints specific mechanistic failures—most clearly, a faster decay of radial position information and increased susceptibility to interference—that underlie the characteristic visuospatial deficits in these conditions.

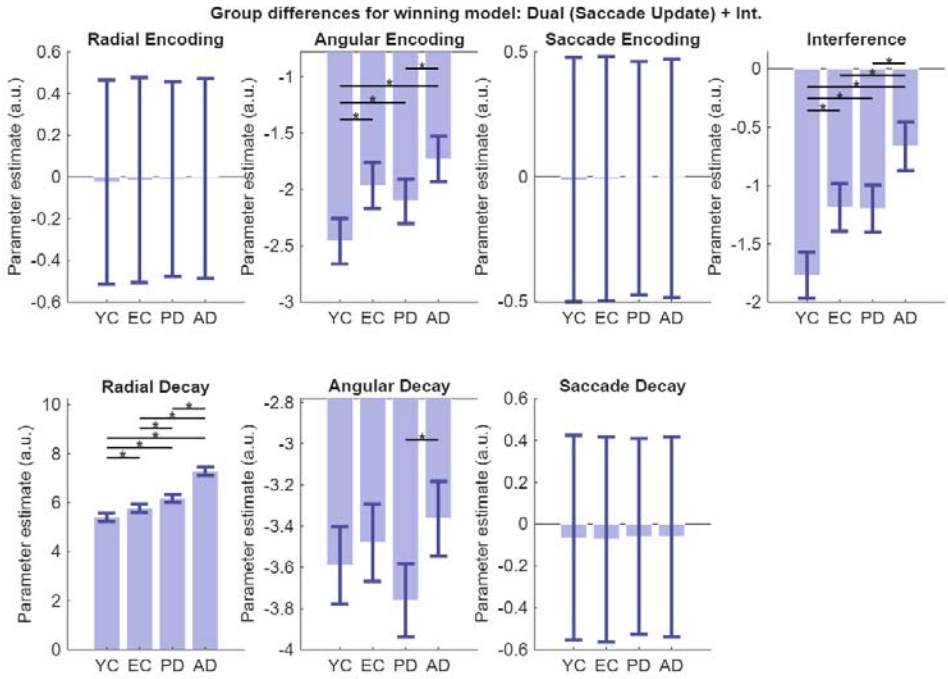

Figure 6: Group differences in winning model parameters.

The plots show group-level parameter estimates from the Parametric Empirical Bayes (PEB) analysis for the winning 'Dual (Saccade) + Interference' model. The y-axis represents the posterior mean of the log-scaled parameter, where a more positive value indicates a greater influence of that parameter on performance (i.e., greater error or faster decay). The exception is the interference parameter, which is effectively a logit parameter, meaning the probability of selecting the distractor is obtained by a sigmoid transform. Error bars represent the 90% posterior confidence intervals. Group differences are indicated by an asterisk (*) if the posterior probability of a difference between the respective parameter estimates is greater than 95%, as calculated from their posterior distributions (i.e., if P(A>B)>0.95 or P(B>A)>0.95). The analysis reveals that Angular Encoding, Angular Decay, Radial Decay, and Interference parameters differentiate the groups. Notably, parameters related to saccade processing (Saccade Encoding and Saccade Decay) and Radial Encoding do not differ between groups.

Transsaccadic working memory predicts copying deficits

To assess how the mechanistic parameters derived from the LOCUS task predict real-world visuospatial abilities, we also instructed all participants to complete the Rey-Osterrieth Complex Figure copy task (ROCF; ***Figure 7A***) on an Android tablet using a digital pen (see examples in ***Figure 7B***; all Copy data are available in the open dataset: https://osf.io/95ecp/).

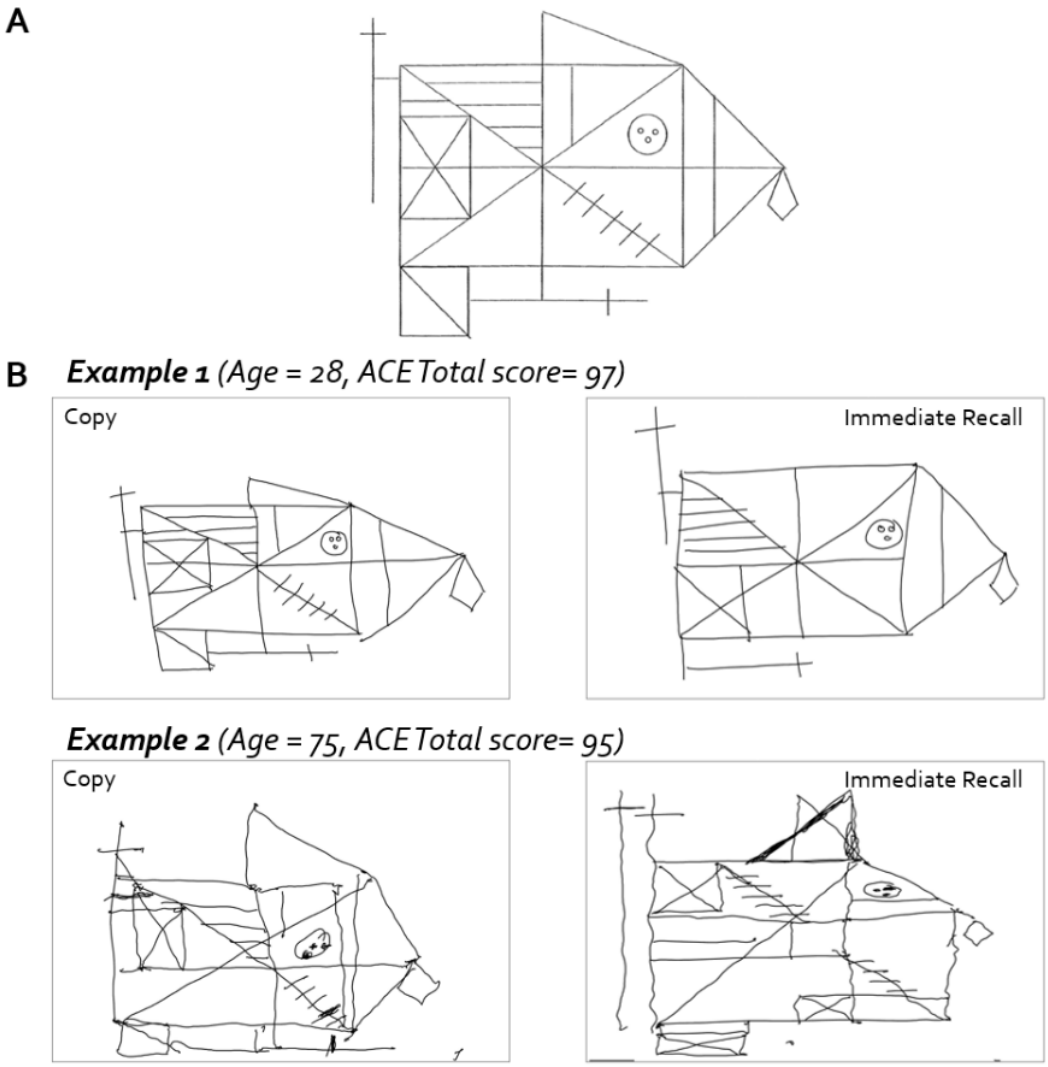

Figure 7: Rey-Osterrieth Complex Figure (ROCF) copying performance.
(A) The original figure that participants copied and recalled. (B) Examples of ROCF copy and immediate recall tasks from a young and an elderly healthy participant, both with normal cognitive function (ACE total score > 88). ACE = Addenbrooke's Cognitive Examination-III.

To assess the ecological validity of the identified saccade-updating retinotopic mechanism, we modelled individual ROCF copy scores across all four groups using the estimated (maximum a posteriori) parameters from the winning "Dual (Saccade) + Interference" model (Model 7; **Figure 8**) as regressors in a Bayesian linear model. Each regressor was normalised by dividing by the square root of its variance. The model successfully explained a significant proportion of the variance in ROCF copy scores (61.99%), indicating that the identified computational mechanisms are strong predictors of constructional ability (**Figure 8A**). The posterior covariance matrix of the regression coefficients associated with each of the model parameters is shown in **Figure 8B**.

Figure 8C indicates how specific mechanistic parameters during transsaccadic working memory contributed to explaining ROCF copy performance. Although as shown in Figure 6, the saccade encoding error did not differentiate across these four groups, it does contribute to a worse ROCF copying performance. This highlights the critical role of accurate

remapping based on saccadic information; even if the core saccadic update mechanism is preserved across groups (as shown in previous analyses), the precision of this updating process is crucial for complex visuospatial tasks. Moreover, worse ROCF copy performance is associated particularly with higher initial angular encoding error. This indicates that imprecision in the initial registration of angular spatial information contributes to difficulties in accurately reproducing complex visual stimuli.

Surprisingly, **less** angular decay was associated with **poorer** ROCF copy scores. However, a plausible explanation for this could be related to the trend seen in angular encoding error. People who have smaller angular encoding error have more “room” for memory decay before angular encoding error accumulates. Evidence for this explanation is evident in the (weak) negative correlation evident in the covariance matrix in Figure 8 between the coefficients for angular encoding and decay rates. The implication is that the results would be similar if we slightly increased the encoding variance while reducing the decay rate, and vice versa.

Conversely, parameters such as radial encoding error, radial decay, saccade decay and interference did not predict ROCF copy scores. This differential predictive power underscores the specific relevance of angular and saccade-related precision for the demanding task of copying complex figures, which inherently requires continuous and accurate spatial updating across multiple fixations.

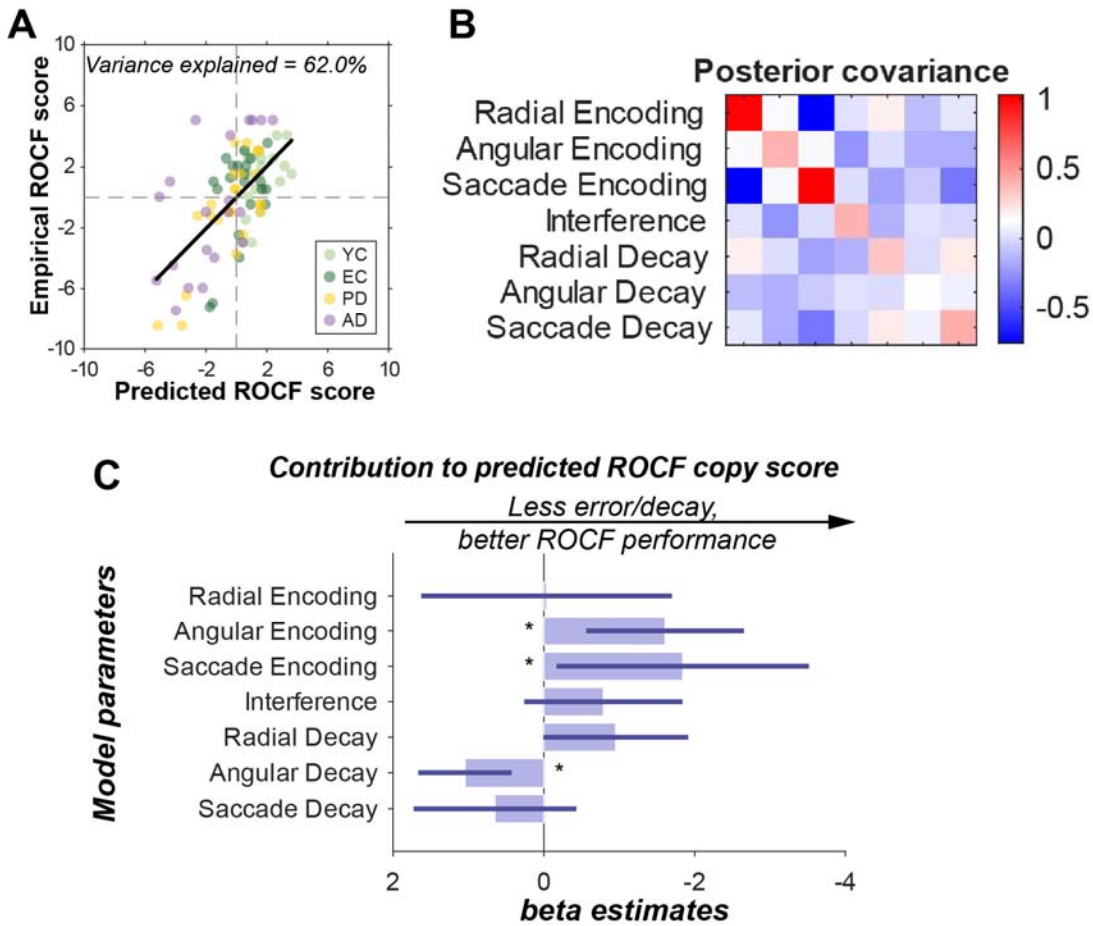

Figure 8: Effect of model parameters on Rey-Osterrieth Complex Figure copy scores.
How model parameters from the wining "Dual (Saccade) + Interference" model explain variance in ROCF copy performance? (A) Predicted versus empirical scores. A scatter plot of empirical ROCF scores against scores predicted by the fitted linear model. Each point represents an individual participant, coloured by diagnostic group: young controls (YC; light green), elderly controls (EC; dark green), Parkinson's disease (PD; yellow), and Alzheimer's disease (AD; purple). A black line denotes the linear fit across all data. ROCF scores were demeaned across participants. Scores outside of 2 standard deviations from the mean were omitted. The plot title indicates the percentage of variance in ROCF copy scores explained by the model. (B) Posterior covariance matrix. A heatmap depicting the posterior covariance between the estimated model parameters (i.e., between the regression coefficients that determine the contribution of each of the parameters from our previous winning model to the ROCF score). Diagonal elements represent individual parameter variances; off-diagonal elements show covariances between parameter pairs. The colour bar provides the scale. (C) Estimated parameter contributions. Bar plot displaying the estimated contribution (beta coefficients) of each LOCUS model parameter to the predicted ROCF copy score. Error bars represent 90% credible intervals (1.65 standard deviations of the posterior variance). Asterisks (∗) denote parameters whose 90% confidence interval does not encompass zero.

Discussion

This study introduced a novel paradigm, the LOCUS task (***Figure 1***), and combined this with computational modelling to investigate the underlying mechanisms and sources of potential errors in dynamic spatial working memory, particularly how the brain maintains a stable world-centred frame of reference across saccades. We investigated this across four cohorts: young healthy adults (YC), healthy elderly adults (EC), and patients with and Alzheimer's disease (AD) and Parkinson's disease (PD). The two clinical groups are known to are frequently associated with significant disruptions to visuospatial processing and oculomotor control [18,19].

The LOCUS task was designed to dissociate retinotopic (within-fixation) and transsaccadic (across-fixation) working memory, examining the precision of both location and colour information maintained across saccades. Our findings reveal a "saccade cost"—a reduction in spatial memory precision following eye movements, consistent with previous research on healthy young adults [20]. Unexpectedly, this saccade cost was remarkably consistent across all four populations, demonstrating its stability with aging and neurodegeneration. This finding implies that any observed reduction in transsaccadic performance in older adults and neurodegenerative patients is primarily attributable to lower baseline retinotopic memory rather than an increased cost associated with saccadic remapping.

The conclusion was further supported by our computational modelling. The winning model, "Dual (Saccade) + Interference", posits an eye-centred, retinotopic representation (encoding stimulus as angular and radial displacement from fixation) that also incorporates saccade-based updating and interference. Although saccade updating was an essential component of the winning model, its two key parameters—initial encoding error and decay rate during maintenance—did not significantly differ across groups. This indicates that the core computational process of updating spatial information based on eye movements is largely preserved in healthy aging and neurodegeneration. Group differences were instead driven by deficits in angular encoding error (precision of initial angle from fixation), angular decay, radial decay (decay in memory of distance from fixation), and interference susceptibility. The eye-centred retinotopic representation is consistent with findings in posterior parietal cortex neurons [27,28] which are considered to play a crucial role in visual localisation as well as remapping across eye movements [9,29]. In using this computational approach, we align our work with established practices in computational psychiatry: Our framework employs Variational Laplace, a method used to recover computational phenotypes in clinical populations like those with substance use disorders [30,31], and features a time-dependent parameterisation of variance conceptually similar to the widely-used Hierarchical Gaussian Filter [32–35].

A clear finding was the specificity of the saccade cost to spatial features; it was not observed for non-spatial features like colour, even in neurodegenerative conditions. This discrepancy challenges notions of fixed visual working memory capacity unaffected by saccades [15,36–38]. The differential impact on spatial versus non-spatial features in transsaccadic memory aligns with the established "what" and "where" pathways in visual processing [39,40]. For objects to remain unified, object features must be bound to stable representations of location across saccades [41]. One possibility is that remapping updates both features and location through a shared mechanism, predicting equal saccadic interference for both colour and location in the present study. However, our findings suggest otherwise. An alternative is that features like colour might be automatically remapped, preserving a coarse representation of the remembered item across saccades [11,42]. Our paradigm offers a tool to further investigate transsaccadic working memory and its capacity across different object features.

Furthermore, we demonstrated that a combination of transsaccadic and retinotopic working memory precision predicts drawing performance on the Rey-Osterrieth Complex Figure (ROCF) copying task. Specifically, higher saccade encoding error and angular encoding error significantly contributed to poorer ROCF copy performance. This highlights the crucial

role of accurate spatial updating and remapping visual representations across retinotopic coordinates for successful visuomotor integration, such as drawing. This link provides insights into the functional role of spatial remapping in everyday cognition. While spatial remapping is often invoked to explain perceptual stability [11–14], the necessity of high-resolution transsaccadic memory for basic visual perception is debated [13,43–45]. A prevailing view suggests that detailed internal models are unnecessary for perception, given the continuous availability of visual information in the external world [13,36]. Our findings support an alternative perspective, aligning with the proposal that high-resolution transsaccadic memory primarily serves action rather than perception [13]. This is consistent with the need for precise localisation in eye-hand coordination tasks such as pointing or grasping [46]. Even when unaware of intrasaccadic target displacements, individuals rapidly adjust their reaching movements, suggesting direct access of the motor system to remapping signals [47]. Further support comes from evidence that pointing to remembered locations is biased by changes in eye position [48], and that remapping neurons reside within the dorsal “action” visual pathway, rather than the ventral “perception” visual pathway [13,49,50]. By demonstrating a strong link between transsaccadic working memory and drawing (a complex fine motor skill), our findings suggest that precise visual working memory across eye movements plays an important role in complex fine motor control.

The results of this study also provide novel insights into the cognitive processes underlying drawing, specifically highlighting the role of transsaccadic working memory in the ability to copy a drawing. Previous research has primarily focused on the roles of fine motor control and eye-hand coordination in this skill [4,51–56]. This is partly because of consistent failure to find a strong relation between memory and drawing or copying ability [4,57]. A recent study highlighted this lack of relationship, by examining ROCF copy performance and various cognitive functions using established neuropsychological battery amongst 142 young children [57]. Despite finding a strong correlation between eye-hand coordination and copying performance, common measures of working memory, such as digit span and Corsi block tasks, did not directly predict copying performance. This seemingly counterintuitive finding suggests that the capacity to maintain information about digits or spatial positions in a sequence does not significantly explain the variance in drawing ability.

This aligns with the seminal study on 3D-block-copying, where participants were found to rarely memorise the entire model [4]. Instead, they focused on information around the block they were actively working on, relying on frequent eye and hand movements to complete the copy. This strategy minimizes the load on traditional working memory but increases the demand for precise eye-hand coordination, a pattern also observed in art students copying complex lines [58]. A commonly accepted explanation for this strategy is that, essentially, when a model is constantly available “out there,” there is no need to construct and maintain a detailed internal representation in memory. Nevertheless, the findings presented here indicate that even with the visual information readily available, drawing still might depend on working memory *across saccades*. In general, such a proposal is consistent with the idea that individuals adapt their gaze and memory strategies based on task demands [3,59]. The results of the studies presented here suggest that there is a specific contribution of working memory to the complex skill of copying a drawing. This may have important implications for understanding how drawing skills are acquired and develop, and for investigating mechanisms underlying drawing deficits observed in clinical populations, e.g. with constructional apraxia, characterised by impaired drawing and copying abilities [60,61].

Materials and Methods

Ethics

The study was performed in accordance with the ethical standards as laid down in the 1964 Declaration of Helsinki and its later amendments. Ethical approval was granted by the University of Oxford ethics committee (IRAS ID: 248379, Ethics Approval Reference: 18/SC/0448). All participants gave written informed consent prior to the start of the study.

Participants

A total of 42 healthy volunteers (21 young adults, mean age = 24.1 years; 21 older adults, mean age = 72.4 years) participated in this study. Their demographics are shown in ***Table 1***. All participants were recruited locally in Oxford, UK, and none were professional artists. Young participants were recruited through the online system of the Department of Experimental Psychology at the University of Oxford. Older adults were recruited from a pool of volunteers registered with the Oxford Dementia and Ageing Research (OxDARE). None of the participants had a psychiatric or neurological illness or was on psychoactive medications. Older adult participants were all over 50 years of age. All participants completed the Addenbrooke's Cognitive Examination-III (ACE) to assess their overall cognitive function [62]. Except for one elderly participant who scored 85, all participants scored above the standard normal cut-off 88.

Group	N	Age	Gender (N of Females)	Handedness (N of Right handed)	Education (Years)	ACE Total
YC	21	24.1 (4.7)	15 (71.4%)	18 (85.7%)	17.0 (2.0)	96.6 (2.9)
EC	21	72.4 (6.3)	12 (57.1%)	18 (85.7%)	16.6 (4.9)	96.1 (3.5)
PD	22	70.7 (6.4)	10 (45.5%)	20 (90.9%)	15.9 (3.3)	93.6 (5.0)
AD	22	68.1 (9.5)	10 (45.5%)	17 (77.3%)	14.7 (4.1)	78.6 (12.7)

Table 1: Demographics of Participants.

The value in brackets indicate one standard deviation or proportion of the sample. YC = Young healthy control; EC = Elderly healthy control; PD = Parkinson's Disease; AD = Alzheimer's Disease; ACE = the Addenbrooke's Cognitive Examination III.

Experimental Procedure

The LOCUS task (LOcation and COlour Updating across Saccades, ***Figure 1***) assessed visuospatial working memory across eye movements. Participants viewed two sequentially presented coloured squares (1-second duration each, with a 0.5-second inter-stimulus interval), memorising their location and colour within frames cantered on a fixation cross. A labelled colour wheel then cued recall of a specific square. Participants selected the remembered colour and dragged a corresponding square to its original screen location.

Saccade demands were manipulated by varying the location of the second frame and colour wheel. In 50% of trials, the second frame appeared in the same location as the first (no saccade required), while in the other 50%, it appeared in a different location, requiring a saccade of at least 8.5° (degrees of visual angle). The colour wheel also appeared in the same or a different location as the second frame with equal probability. This creates four conditions: No-saccade, Saccade-After-Item 1, Saccade-After-Item-2, or Two-Saccades (***Figure 1***). Each condition comprised 25% of the 160 trials, presented in 16 randomised blocks.

The coloured square was 0.66° × 0.66° visual angle, the fixation cross was 1° × 1° visual angle, and the frame was 9.8° × 9.8° visual angle with a 0.1° linewidth. The location of the square was randomised within the frame with a fixed minimal distance from fixation cross of 3.82° visual angle. The screen had 3 x 5 possible frame locations with a 0.3° gap between

frames. The colour wheel was 4.5° wide, with a 1.5°-wide inner black circle displaying a 1° tall label (probing “1” or “2”). The colour and location of squares were generated pseudorandomly for each participant just before the starting experiment. To avoid the potential bias to certain locations on the colour wheel, the colour wheel’s rotation was randomised for every trial.

Participants were instructed to maintain fixation on a cross when it was present, and to execute saccades to peripheral targets when prompted by appearance of a new frame at a different location or the appearance of the colour wheel. When item 1 or 2 was displayed, it was positioned within a square frame with a central fixation cross (***Figure 2***). The use of a square frame and central fixation cross served to emphasise the retinotopic reference frame, highlighting no need to move the eyes unless these elements were extinguished, and a new stimulus appeared in the periphery. Thus, in the no-saccade condition, participants did not need to make eye movements and therefore respond without having to rely on transsaccadic memory.

To mitigate potential confounds related to visual impairment or inability to fixate with task instructions, we monitored eye position throughout the experiment. Eye-tracking analysis confirmed high compliance: participants fixated the cross in the majority of trials (81% ± 10%), with no significant difference between age groups ($t(40) = 0.76$, $p = 0.45$). Fixation durations averaged 0.21s (± 0.05s), sufficient for encoding visual information. Furthermore, in the no-saccade condition, participants successfully maintained fixation in 80% of trials (± 10%). Similarly, in the saccade conditions, participants accurately executed saccades away when required on 86% of trials (± 18%). Non-compliance trials were excluded from further analysis.

Measurement of Saccade Cost

The LOCUS task allows for the quantification of several key metrics: (1) retinotopic working memory: the location error in no-saccade condition, (2) transsaccadic working memory: the location error in two-saccades condition, and (3) “saccade cost”: the reduction in spatial memory accuracy attributable to saccades. Whie a straightforward approach to quantify saccade cost would be to directly compare performance in the two-saccades condition to the no-saccade condition, this method confounds saccade cost with retinotopic working memory. To isolate the effect of saccades on memory independent of retinotopic condition, we calculated saccade cost as the difference in performance between the Two-Saccade condition and the Saccade-After-The-Other-Item condition. This yields a specific measure of the additional memory error due to a saccade made immediately after the probed item.

Furthermore, we conducted a secondary analysis using the beta coefficient derived from a multiple linear regression model to estimate the effect of saccades and item order on location errors. This approach confirmed the relationship between saccade cost and ROCF copy performance, demonstrating the robustness of our findings.

Rey-Osterrieth Complex Figure (ROCF)

Participants completed the ROCF copy and immediate recall tasks on a Galaxy Tab S3 tablet (SM-T820) using the corresponding digital pen (Galaxy Tab S3 S Pen). The tablet's screen dimensions were 148 x 197 mm (1536 x 2048 pixels, 264 ppi density). Participants placed the tablet on the table upright. During the copy phase, the ROCF figure displayed on the top of the tablet [63]. They first copied the figure in the lower portion of the screen. Upon completion, they were instructed to reproduce the ROCF from memory, without the figure present. Drawing traces were recorded and printed for blind scoring by two experienced raters using the standard 18-element scoring system [64].

For further analysis, the drawing paths were analysed in MATLAB using in-house scripts. We extracted the total time taken to complete each task, calculated from the first moment the

digital pen touched the screen to the final pen lift. In addition, we extracted total distance drawn (total path length in pixels), path drawing speed (mean derivative of path distance per second), and mean waiting time (duration between completing the last path and starting the next path).

Methods – Computational Modelling

We used of series of simple computational models to test a set of hypotheses about the mechanisms that underwrite the measured data. All hypotheses rely upon the idea that memory decays with time since the stimulus was presented, modelled here using a diffusion (or Brownian motion) like process. Under this formulation, the shape of the distribution of expected responses, and its change over time, will depend upon the way in which our brains represent the variables that we expect to decay. Conceptually, our hypotheses distinguished between allocentric (screen centred) coordinates and retinotopic coordinates, whether target and distractor representations do or do not interfere with one another, whether there was evidence for an embodied representation in which the current position of the eyes helps reinforce a memory and, if so, whether remembered locations are centred on remembered fixations or on relative position based upon memories of the vectors of saccades performed since that location.

Figure 9 shows the form of these hypotheses, each of which can be expressed with a time-dependent likelihood function. Each of these models was fit to the responses made by each participant, where the response data were rotated and translated such that the target stimulus was always in the same angle, and the origin was always set to be the fixation location associated with the probed stimulus. The model fits were performed using a Variational Laplace procedure (a form of approximate Bayesian inference) using a Newton optimisation scheme as implemented in SPM25 using the spm_nlsi_Newton.m MATLAB routine.[65,66] This relies upon a specification of a log likelihood function which gives the distribution, given the parameters, of the recorded responses. In the allocentric model, this log likelihood function had the form:

$$\mathcal{L}(\boldsymbol{\kappa}) = ln\big(\mathcal{N}(u; x, \kappa_1\tau + \kappa_2) \times \mathcal{N}(v; y, \kappa_1\tau + \kappa_2)\big)$$

Here, (u,v) are the Euclidean coordinates of the response to a stimulus presented at coordinates (x,y), with an encoding variance of κ_2 and a decay constant of κ_1 which scales with the time τ between the stimulus presentation and the response. This is summed over all responses a participant has made accounting for the time at which they are made to give the accumulated log likelihood for the parameters for that dataset.

The dual models, with a retinotopic component, all have the form:

$$\mathcal{L}(\boldsymbol{\kappa}) = ln\left(\mathcal{N}\left(\sqrt{(u-x)^2 + (v-y)^2}; r, \Sigma_r(\kappa, \tau, t, T)\right) \times \mathcal{N}\left(\tan^{-1}\left(\frac{v-y}{u-x}\right); \theta, \Sigma_\theta(\kappa, \tau, t, T)\right)\right)$$

Here, the principle is similar, but the distributions are over the polar coordinates of the response, with (r,θ) representing the polar coordinates of the stimulus. The variances, Σ, are functions now of the parameter set and (up to) three different time variables. These different times are illustrated schematically in Figure X (middle panel) and are disambiguated by the different experimental conditions. They are:

1. the time since the stimulus was visible (τ)
2. the time since the first saccade (if any) since the stimulus was present (t)
3. the time since the second saccade (if any) after the stimulus (T).

The forms of the variance functions are shown in Figure X. Here we see a combination of encoding parameters (time-independent), and decay parameters for retinotopic stimulus memories (multiplied by τ), fixation locations (multiplied by t) and saccade vectors (multiplied

by $t + T$). The reason for multiplying saccade decay constants by the sum of t and T is that a reconstructed fixation location based upon saccade vectors will have a cumulative increase in uncertainty with each saccade since that fixation.

Finally, the likelihood for the interference models is the weighted sum of two likelihood ($e^{\mathcal{L}(\kappa)}$) functions of the form above, but with one computed from the target location and the other from the distractor location. The interference parameter determined the weighting towards the distractor.

We used relatively conservative priors, which were (for all parameters) normal distributions centred on zero, with a spherical covariance of 1/8. This ensured we needed good evidence for the parameters to be estimated as being confidently non-zero. All parameters were log scaling parameters (ensuring the scaling parameters were positive) except for the interference parameter, when present, which was passed through a sigmoid function to constrain the effect of the parameter to lie between zero and one.

Variational Laplace provides approximate Bayesian model evidence values, and posterior probability distributions for each parameter, for each model and participant. By accumulating the log model evidence across all participants and applying a softmax function, we arrived at posterior probabilities for each model. We selected the winning model for subsequent steps of the analysis. Our next stage was to use Parametric Empirical Bayes (PEB)[67] to assess the effect of diagnostic group on the individual parameter estimates. PEB is effectively a second level linear model. We used the SPM25 implementation spm_dcm_peb.m [65].

Finally, to test hypotheses about the mechanisms that explain performance on complex figure drawing, we took the maximum a posteriori estimates (MAP) for all parameters in the winning model for all participants and used these, normalised by their variance, as regressors for a linear model to predict mean-centred copy scores (omitting those scores > 2 SD from the mean) and changes in score on immediate recall. Again, we used spm_nlsi_Newton.m to invert this linear model. Following inversion, we computed the predicted scores based upon the MAP values of the regression coefficients and assessed the percentage of empirical variance explained. The percentage of empirical variance explained by the model was assessed using the formula: 100×(1−var(residuals)/var(empirical_scores)).

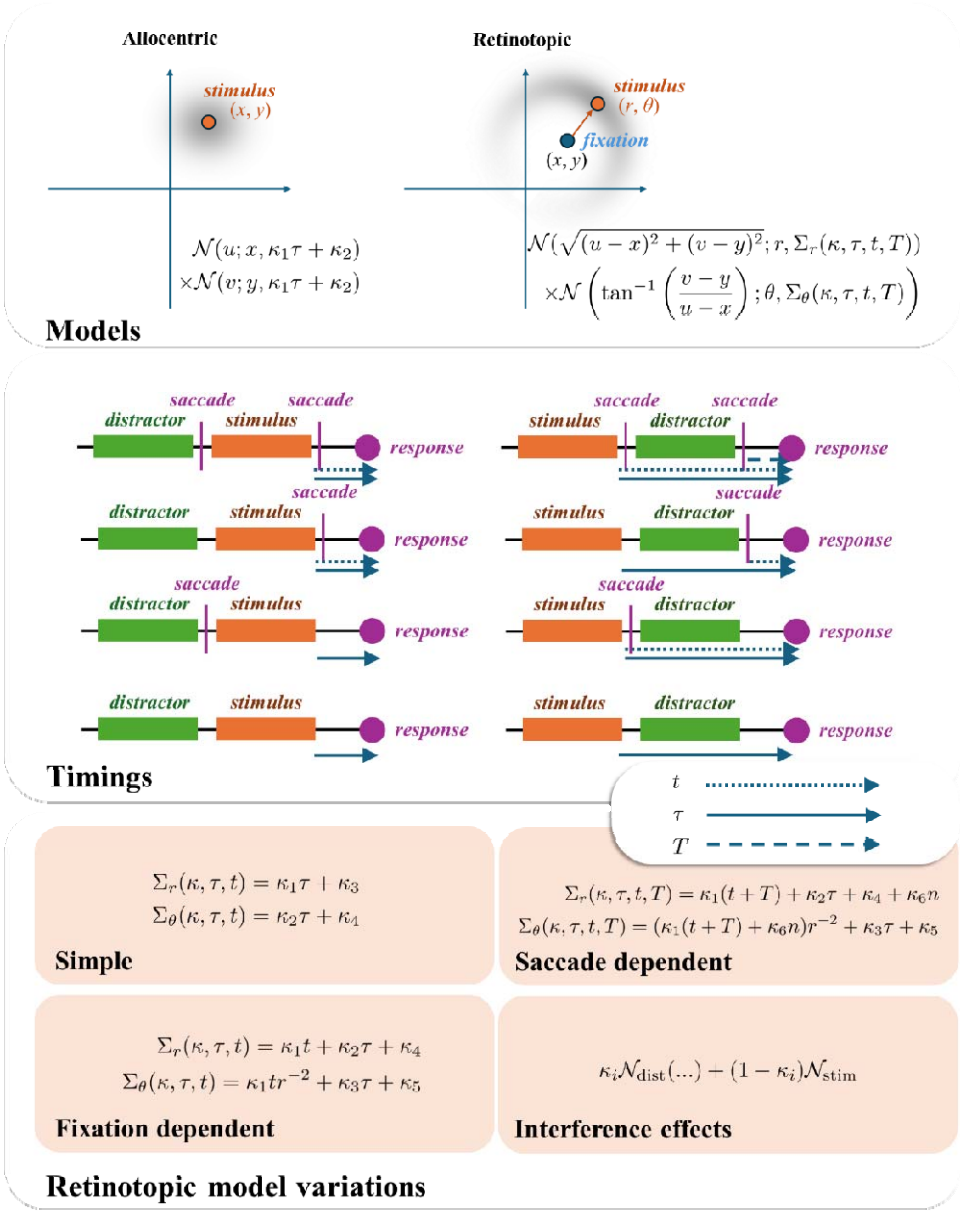

Figure 9: Models and hypotheses.

This figure illustrates the form of the models used for our model comparisons. The upper panel shows the distinction between allocentric screen centred coordinates, which we treat as a decay in Euclidean space, such that the probability density of a response (coordinates (u,v)) is a normal distribution whose covariance grows with time centred on the stimulus. In contrast, the retinotopic representation uses polar coordinates with both radial and angular decays. There are several ways in which the associated covariance can be formulated, and this depends upon the different times over which the decay in memory might occur. The different timings in the alternative experimental conditions are shown schematically in the middle panel, dealing with the time since the stimulus was visible (τ), the time since the first saccade (if any) since the stimulus was present (t), and the time since the second saccade (if any) after the stimulus (T). The variations, based on these timings, for the dynamics of the covariance for the retinotopic model, are shown in the lower panel. The simple model assumes that any decay in the fixation location around which the retinotopic coordinates can be captured by decays in the radial and angular coordinates. This implies there is no difference in the form of the decay when the same fixation location is sustained after the stimulus disappears compared to when a subsequent saccade is made. The fixation-dependent model assumes instead that there is an independent decay in the fixation location, which only begins once we have moved our eyes from the location at which we

saw the stimulus. In contrast, the saccade dependent framing assumes that, rather than retain a memory of fixation location, we reconstruct the fixation location based upon our memory of the saccade vectors made, since that fixation. Here, the n variable represents the number of saccades made since the relevant fixation. The interference effects are mediated by computing the distribution we would expect from a response to the target stimulus and the distribution we would expect from a response to the distractor stimulus (translated into the same retinotopic space) and taking a weighted sum of the two.

Statistical Analysis

All statistical analyses were conducted in MATLAB R2025a and JASP [68]. For correlations, Spearman's rho was reported with two-tailed p-values (alpha = 0.05) and effect size (Fisher's z). Bayesian comparisons were also performed, with Bayes Factor 10 (BF_{10}) reported when applicable. For ANOVAs, Mauchly's test of sphericity was applied, and Greenhouse-Geisser correction was used when sphericity was violated. F-stats, p values, and partial eta-squared were reported. Note that sphericity correction is not available for factors with two levels, such as the item factor (only two items). For multiple comparisons, Bonferroni-corrected p-values (*p*(bonf)) were reported.

Multiple linear regression models were fit for each participant using all trials. The regression analyses were conducted via the MATLAB function *regress*. The resulting beta coefficients were then averaged across participants. A one-sample t-test (two-tailed) was used to determine if the group average beta coefficient for each predictor was significantly different from zero. The t-statistic and p-value (two-tailed) are reported for each predictor.

Mediation analysis with multiple mediators was conducted in JASP, using standardised regression coefficients [68]. The bias-corrected bootstrap method with 1000 iterations was used to estimate confidence intervals for the indirect and direct effects [69].

The bayes factor was computed as the division of accumulated posterior probability between the winning model and the next best alternative.

For comparing group differences in the estimated parameters of the winning model, a parametric empirical Bayes (PEB) approach was utilised, employing spm_dcm_peb in SPM25. This hierarchical Bayesian method allows for robust group-level inference by modelling individual parameter estimates as samples drawn from a group distribution, thereby accounting for inter-subject variability and propagating uncertainty from the first (individual) level. For each parameter of interest, the group-level posterior mean and covariance were obtained from the PEB analysis. To assess statistically significant differences between groups for a given parameter, the probability of a directional difference between the posterior estimates of any two groups was calculated using their respective posterior distributions. A difference was deemed statistically significant if this calculated probability was greater than 0.95 (corresponding to strong evidence in favour of a directional difference).

Eyetracking Recording

Participants sat in front of a 21" CRT computer screen (1024 × 768 pixels; 100 Hz refresh rate) at a viewing distance of 60 cm in a dimly lit quiet room with their head supported on a chinrest. Visual stimuli were presented using MATLAB (The MathWorks) and Psychophysics Toolbox [70,71] on a Windows-XP computer. Eye positions during the LOCUS task were monitored using a frame-mounted infrared eye-tracking camera (Eyelink 1000 Tower Mounted, SR Research Ltd.). Right eye was recorded at a sampling rate of 1000 Hz. A nine-point calibration procedure for the Eyelink system was conducted prior the experiment.

Eyetracking Data Analysis

All eyertracking analysis was performed offline. Interval where the eye tracker detected full and partial eye closures were automatically treated as missing data. Furthermore, intervals

where pupil diameter was recorded as 0 or change dramatically immediately pre- or post-blink were also automatically treated as blinks and removed. Gaze positions were epoched relative to stimulus onset (item 1, item 2 and colour wheel) and analysed for 1 second post-stimulus-onset. Euclidean distance that the gaze travelled to the target was computed and converted to visual degrees. Fixations were defined as gaze remaining within 2.5° of the target for at least 150 ms. Saccades were defined as eye movements exceeding 150° visual angle per second, lasting longer than 10 ms in duration, and traversing a distance greater than 9.2° from the initial fixation. The distance of 9.2° was defined as it is the radius of perifoveal visual field [72,73].

Task compliance was assessed based on fixation and saccade criteria specific to each condition. For example, in the Saccade-After-Item-1 condition, compliance required fixations on both Item 1 and Item 2, with no saccade exceeding 9.2° after Item 2 measured in the epoch after the onset of colour wheel.

References

1. Land MF, Hayhoe M. In what ways do eye movements contribute to everyday activities? Vision Research. 2001;41: 3559–3565. doi:10.1016/S0042-6989(01)00102-X

2. Crawford JD, Medendorp WP, Marotta JJ. Spatial Transformations for Eye–Hand Coordination. Journal of Neurophysiology. 2004;92: 10–19. doi:10.1152/jn.00117.2004

3. Draschkow D, Kallmayer M, Nobre AC. When Natural Behavior Engages Working Memory. Current Biology. 2021;31: 869-874.e5. doi:10.1016/j.cub.2020.11.013

4. Ballard DH, Hayhoe MM, Pelz JB. Memory Representations in Natural Tasks. Journal of Cognitive Neuroscience. 1995;7: 66–80. doi:10.1162/jocn.1995.7.1.66

5. Cohen DJ. Look little, look often: The influence of gaze frequency on drawing accuracy. Perception & Psychophysics. 2005;67: 997–1009. doi:10.3758/BF03193626

6. McManus IC, Chamberlain R, Loo P-W, Rankin Q, Riley H, Brunswick N. Art students who cannot draw: Exploring the relations between drawing ability, visual memory, accuracy of copying, and dyslexia. Psychology of Aesthetics, Creativity, and the Arts. 2010;4: 18–30. doi:10.1037/a0017335

7. Perdreau F, Cavanagh P. Drawing experts have better visual memory while drawing. Journal of Vision. 2015;15: 5. doi:10.1167/15.5.5

8. Grzeczkowski L, Shi Z, Rolfs M, Deubel H. Perceptual learning across saccades: Feature but not location specific. Proceedings of the National Academy of Sciences. 2023;120: e2303763120. doi:10.1073/pnas.2303763120

9. Duhamel J-R, Colby CL, Goldberg ME. The Updating of the Representation of Visual Space in Parietal Cortex by Intended Eye Movements. Science. 1992;255: 90–92. doi:10.1126/science.1553535

10. Colby CL, Goldberg ME. Space And Attention In Parietal Cortex. Annu Rev Neurosci. 1999;22: 319–349. doi:10.1146/annurev.neuro.22.1.319

11. Golomb JD, Mazer JA. Visual Remapping. Annual Review of Vision Science. 2021;7: 257–277. doi:10.1146/annurev-vision-032321-100012

12. Melcher D, Colby CL. Trans-saccadic perception. Trends in Cognitive Sciences. 2008;12: 466–473. doi:10.1016/j.tics.2008.09.003

13. Bays PM, Husain M. Spatial remapping of the visual world across saccades. NeuroReport. 2007;18: 1207–1213. doi:10.1097/WNR.0b013e328244e6c3

14. Harrison WJ, Stead I, Wallis TSA, Bex PJ, Mattingley JB. A computational account of transsaccadic attentional allocation based on visual gain fields. Proc Natl Acad Sci USA. 2024;121: e2316608121. doi:10.1073/pnas.2316608121

15. Irwin DE. Memory for position and identity across eye movements. Journal of Experimental Psychology: Learning, Memory, and Cognition. 1992;18: 307–317. doi:10.1037/0278-7393.18.2.307

16. Golomb JD. Remapping locations and features across saccades: a dual-spotlight theory of attentional updating. Current Opinion in Psychology. 2019;29: 211–218. doi:10.1016/j.copsyc.2019.03.018

17. Schneegans S, Bays PM. Drift in Neural Population Activity Causes Working Memory to Deteriorate Over Time. J Neurosci. 2018;38: 4859–4869. doi:10.1523/JNEUROSCI.3440-17.2018

18. Cormack F, Aarsland D, Ballard C, Tovée MJ. Pentagon drawing and neuropsychological performance in Dementia with Lewy Bodies, Alzheimer's disease, Parkinson's disease and Parkinson's disease with dementia. Int J Geriatr Psychiatry. 2004;19: 371–377. doi:10.1002/gps.1094

19. Trojano L, Gainotti G. Drawing Disorders in Alzheimer's Disease and Other Forms of Dementia. J Alzheimers Dis. 2016;53: 31–52. doi:10.3233/JAD-160009

20. Golomb JD, Kanwisher N. Retinotopic memory is more precise than spatiotopic memory. Proc Natl Acad Sci USA. 2012;109: 1796–1801. doi:10.1073/pnas.1113168109

21. Broadbent DE, Broadbent MHP. Recency effects in visual memory. The Quarterly Journal of Experimental Psychology Section A. 1981;33: 1–15. doi:10.1080/14640748108400762

22. Murdock BB. The serial position effect of free recall. Journal of Experimental Psychology. 1962;64: 482–488. doi:10.1037/h0045106

23. Penny WD. Comparing Dynamic Causal Models using AIC, BIC and Free Energy. Neuroimage. 2012;59: 319–330. doi:10.1016/j.neuroimage.2011.07.039

24. Rasmussen C, Ghahramani Z. Occam' s Razor. Advances in Neural Information Processing Systems. MIT Press; 2000. Available: https://papers.nips.cc/paper_files/paper/2000/hash/0950ca92a4dcf426067cfd2246bb5ff3-Abstract.html

25. MacKay DJC. Information Theory, Inference and Learning Algorithms. Cambridge University Press; 2003.

26. Zeidman P, Jafarian A, Seghier ML, Litvak V, Cagnan H, Price CJ, et al. A guide to group effective connectivity analysis, part 2: Second level analysis with PEB. Neuroimage. 2019;200: 12–25. doi:10.1016/j.neuroimage.2019.06.032

27. Cohen YE, Andersen RA. A common reference frame for movement plans in the posterior parietal cortex. Nat Rev Neurosci. 2002;3: 553–562. doi:10.1038/nrn873

28. Land MF. The Operation of the Visual System in Relation to Action. Current Biology. 2012;22: R811–R817. doi:10.1016/j.cub.2012.06.049

29. Ten Brink AF, Fabius JH, Weaver NA, Nijboer TCW, Van der Stigchel S. Trans-saccadic memory after right parietal brain damage. Cortex. 2019;120: 284–297. doi:10.1016/j.cortex.2019.06.006

30. Smith R, Lavalley CA, Taylor S, Stewart JL, Khalsa SS, Berg H, et al. Elevated decision uncertainty and reduced avoidance drives in depression, anxiety and substance use disorders during approach–avoidance conflict: a replication study. Journal of Psychiatry and Neuroscience. 2023;48: E217–E231. doi:10.1503/jpn.220226

31. Taylor S, Lavalley CA, Hakimi N, Stewart JL, Ironside M, Zheng H, et al. Active learning impairments in substance use disorders when resolving the explore-exploit dilemma: A replication and extension of previous computational modeling results. Drug and Alcohol Dependence. 2023;252: 110945. doi:10.1016/j.drugalcdep.2023.110945

32. Mathys CD, Lomakina EI, Daunizeau J, Iglesias S, Brodersen KH, Friston KJ, et al. Uncertainty in perception and the Hierarchical Gaussian Filter. Front Hum Neurosci. 2014;8. doi:10.3389/fnhum.2014.00825

33. Hess AJ, Iglesias S, Köchli L, Marino S, Müller-Schrader M, Rigoux L, et al. Bayesian Workflow for Generative Modeling in Computational Psychiatry. Comput Psychiatr. 2025;9: 76–99. doi:10.5334/cpsy.116

34. Marshall L, Mathys C, Ruge D, Berker AO de, Dayan P, Stephan KE, et al. Pharmacological Fingerprints of Contextual Uncertainty. PLOS Biology. 2016;14: e1002575. doi:10.1371/journal.pbio.1002575

35. Kirsch LP, Mathys C, Papadaki C, Talelli P, Friston K, Moro V, et al. Updating beliefs beyond the here-and-now: the counter-factual self in anosognosia for hemiplegia. Brain Communications. 2021;3. doi:10.1093/braincomms/fcab098

36. Prime SL, Vesia M, Crawford JD. Cortical mechanisms for trans-saccadic memory and integration of multiple object features. Philosophical Transactions of the Royal Society B: Biological Sciences. 2011 [cited 25 Sept 2024]. doi:10.1098/rstb.2010.0184

37. Prime SL, Tsotsos L, Keith GP, Crawford JD. Visual memory capacity in transsaccadic integration. Exp Brain Res. 2007;180: 609–628. doi:10.1007/s00221-007-0885-4

38. Irwin DE, Gordon RD. Eye Movements, Attention and Trans-saccadic Memory. Visual Cognition. 1998;5: 127–155. doi:10.1080/713756783

39. Ungerleider LG, Mishkin M. Two cortical visual systems. Analysis of visual behavior. Cambridge, MA, USA: MIT Press; 1982. pp. 549–586.

40. Mishkin M, Ungerleider LG, Macko KA. Object vision and spatial vision: two cortical pathways. Trends in Neurosciences. 1983;6: 414–417. doi:10.1016/0166-2236(83)90190-X

41. Cavanagh P, Hunt AR, Afraz A, Rolfs M. Visual stability based on remapping of attention pointers. Trends in Cognitive Sciences. 2010;14: 147–153. doi:10.1016/j.tics.2010.01.007

42. Fabius JH, Fracasso A, Acunzo DJ, Stigchel SV der, Melcher D. Low-Level Visual Information Is Maintained across Saccades, Allowing for a Postsaccadic Handoff between Visual Areas. J Neurosci. 2020;40: 9476–9486. doi:10.1523/JNEUROSCI.1169-20.2020

43. Irwin DE, Yantis S, Jonides J. Evidence against visual integration across saccadic eye movements. Perception & Psychophysics. 1983;34: 49–57. doi:10.3758/BF03205895

44. Irwin DE, Brown JS, Sun J. Visual masking and visual integration across saccadic eye movements. Journal of Experimental Psychology: General. 1988;117: 276–287. doi:10.1037/0096-3445.117.3.276

45. Rayner K, McConkie GW, Zola D. Integrating information across eye movements. Cognitive Psychology. 1980;12: 206–226. doi:10.1016/0010-0285(80)90009-2

46. Baltaretu BR, Monaco S, Velji-Ibrahim J, Luabeya GN, Crawford JD. Parietal Cortex Integrates Saccade and Object Orientation Signals to Update Grasp Plans. The Journal of Neuroscience. 2020;40. doi:10.1523/jneurosci.0300-20.2020

47. Prablanc C, Martin O. Automatic control during hand reaching at undetected two-dimensional target displacements. J Neurophysiol. 1992;67: 455–469. doi:10.1152/jn.1992.67.2.455

48. Henriques DYP, Klier EM, Smith MA, Lowy D, Crawford JD. Gaze-Centered Remapping of Remembered Visual Space in an Open-Loop Pointing Task. J Neurosci. 1998;18: 1583–1594. doi:10.1523/JNEUROSCI.18-04-01583.1998

49. Husain M, Nachev P. Space and the parietal cortex. Trends in Cognitive Sciences. 2007;11: 30–36. doi:10.1016/j.tics.2006.10.011

50. Goodale MA, Westwood DA. An evolving view of duplex vision: separate but interacting cortical pathways for perception and action. Current Opinion in Neurobiology. 2004;14: 203–211. doi:10.1016/j.conb.2004.03.002

51. Cohen EJ, Bravi R, Minciacchi D. Assessing the Development of Fine Motor Control in Elementary School Children Using Drawing and Tracing Tasks. Percept Mot Skills. 2021;128: 605–624. doi:10.1177/0031512521990358

52. Raimo S, Santangelo G, Trojano L. The Neural Bases of Drawing. A Meta-analysis and a Systematic Literature Review of Neurofunctional Studies in Healthy Individuals. Neuropsychol Rev. 2021;31: 689–702. doi:10.1007/s11065-021-09494-4

53. Trojano L, Grossi D, Flash T. Cognitive neuroscience of drawing: Contributions of neuropsychological, experimental and neurofunctional studies. Cortex. 2009;45: 269–277. doi:10.1016/j.cortex.2008.11.015

54. Bai S, Liu W, Guan Y. The Visuospatial and Sensorimotor Functions of Posterior Parietal Cortex in Drawing Tasks: A Review. Front Aging Neurosci. 2021;13. doi:10.3389/fnagi.2021.717002

55. Gowen E, Miall RC. Eye–hand interactions in tracing and drawing tasks. Human Movement Science. 2006;25: 568–585. doi:10.1016/j.humov.2006.06.005

56. Petilli MA, Daini R, Saibene FL, Rabuffetti M. Automated scoring for a Tablet-based Rey Figure copy task differentiates constructional, organisational, and motor abilities. Sci Rep. 2021;11: 14895. doi:10.1038/s41598-021-94247-9

57. Senese VP, Zappullo I, Baiano C, Zoccolotti P, Monaco M, Conson M. Identifying neuropsychological predictors of drawing skills in elementary school children. Child Neuropsychology. 2020;26: 345–361. doi:10.1080/09297049.2019.1651834

58. Tchalenko J, Chris Miall R. Eye–hand strategies in copying complex lines. Cortex. 2009;45: 368–376. doi:10.1016/j.cortex.2007.12.012

59. Droll JA, Hayhoe MM. Trade-offs between gaze and working memory use. Journal of Experimental Psychology: Human Perception and Performance. 2007;33: 1352–1365. doi:10.1037/0096-1523.33.6.1352

60. Russell C, Deidda C, Malhotra P, Crinion JT, Merola S, Husain M. A deficit of spatial remapping in constructional apraxia after right-hemisphere stroke. Brain. 2010;133: 1239–1251. doi:10.1093/brain/awq052

61. Van der Stigchel S, de Bresser J, Heinen R, Koek HL, Reijmer YD, Biessels GJ, et al. Parietal Involvement in Constructional Apraxia as Measured Using the Pentagon Copying Task. Dementia and Geriatric Cognitive Disorders. 2018;46: 50–59. doi:10.1159/000491634

62. Mathuranath PS, Nestor PJ, Berrios GE, Rakowicz W, Hodges JR. A brief cognitive test battery to differentiate Alzheimer's disease and frontotemporal dementia. Neurology. 2000;55: 1613–1620. doi:10.1212/01.wnl.0000434309.85312.19

63. Rey A. L'examen psychologique dans les cas d'encephalopathie traumatique. Archives de Psychologie. 1941;28: 286–340.

64. Osterrieth PA. Le test de copie d'une figure complexe; contribution à l'étude de la perception et de la mémoire. Archives de Psychologie. 1944;30: 206–356.

65. Tierney TM, Alexander NA, Avila NL, Balbastre Y, Barnes G, Bezsudnova Y, et al. SPM 25: open source neuroimaging analysis software. arXiv; 2025. doi:10.48550/arXiv.2501.12081

66. Zeidman P, Friston K, Parr T. A primer on Variational Laplace (VL). NeuroImage. 2023;279: 120310. doi:10.1016/j.neuroimage.2023.120310

67. Friston KJ, Litvak V, Oswal A, Razi A, Stephan KE, van Wijk BCM, et al. Bayesian model reduction and empirical Bayes for group (DCM) studies. NeuroImage. 2016;128: 413–431. doi:10.1016/j.neuroimage.2015.11.015

68. JASP Team. JASP. 2024.

69. Biesanz JC, Falk CF, Savalei V. Assessing Mediational Models: Testing and Interval Estimation for Indirect Effects. Multivariate Behavioral Research. 2010;45: 661–701. doi:10.1080/00273171.2010.498292

70. Brainard DH. The Psychophysics Toolbox. Spat Vis. 1997;10: 433–436. doi:https://doi.org/10.1163/156856897X00357

71. Kleiner M, Brainard D, Pelli D, Ingling A, Murray R, Broussard C. What's new in psychtoolbox-3. Perception. 2007;36: 1–16.

72. Polyak SL. The Retina. Chicago: University of Chicago Press; 1941.

73. Sakurai M. Parafovea. In: Shamey R, editor. Encyclopedia of Color Science and Technology. Berlin, Heidelberg: Springer; 2020. pp. 1–3. doi:10.1007/978-3-642-27851-8_215-2